

# Practical Approach of Penetration Index Equations for Use in BOF Blowing Pattern Design



## Authors

**Breno Totti Maia** (top row, left)  
BOF technical director, Lumar Metals,  
Belo Horizonte, MG, Brazil  
breno.totti@lumarmetals.com.br

**Roberto Parreiras Tavares**  
(top row, right)  
professor, Universidade Federal de  
Minas Gerais, Belo Horizonte,  
MG, Brazil  
rtavares@demet.ufmg.br

**Shank Balajee** (bottom row, left)  
retired, ArcelorMittal Indiana Harbor,  
Highland, Ind., USA  
balajee@att.net

**Jürgen Cappel** (bottom row, right)  
iron- and steelmaking consultant,  
CSC Cappel Stahl Consulting GmbH,  
Meerbusch, Germany  
juergen.cappel@cappel-consult.com

Considering a dimensionless parameter  $L/L_0$ , where  $L_0$  is the liquid steel bath height, this paper will critically review both the theoretical and practical aspects of these depth of penetration equations, and recommend the most feasible equation(s) to determine the lance gap to use during the oxygen blow. Further, the effects of the penetration depth, like total surface of the penetration cavity, which is the reaction surface for direct reaction of oxygen with the metal bath, and droplet generation and size, which is the reaction surface for reaction of Fe droplets with slag FeO, will be discussed.

The basic oxygen process (BOP) for steelmaking uses hot metal, scrap, and flux and refining by oxygen gas. Numerous papers about the process fundamentals and reactions going on during the blow have been published. Numerous lab-scale, half-industrial and industrial trials have been carried out to understand the behavior of the process. All operators of basic oxygen furnaces (BOF) know that the process is still not monitored and controlled completely, and undesired reactions and effects occur on a regular basis. The main problem is, as opposed to fully controlled processes, the controllability of the BOF operation is limited by the fact that it is impossible to look inside the furnace and react to process changes. It is common procedure to operate BOF furnaces by application of charge recipes and blowing patterns.

## BOF Blowing Patterns

The BOF blowing patterns, in general, can be split into the different stages of the process happening one after the other or simultaneously, as described in Table 1.

Starting from ignition, the slag formation by oxidation of  $[\%Fe]$ ,  $[\%Si] + [\%Mn]$  and  $[\%P]$  is the first important phase of the process. In this phase, only little decarburization is observed. In the middle of the blow, as soon as the other

hot metal components have been oxidized to slag, the main decarburization starts in the initial stage with high speed, later at decreasing contents in the bath with lower speed. In the high-speed phase, the consumption of oxygen for decarburization is higher than offered by the blow, so a reduction of the slag ( $\%FeO$ ) occurs, which is accompanied by a simultaneous reduction of ( $\%MnO$ ) and ( $\%P_2O_5$ ) as well. This so-called Mn and P reversion has been proven in many trials with in-blow sampling from various researchers. The decarburization rate can be maintained by increasing the jet force until toward the end of the blow, where the rate collapses. At this point, endpoint control models based on offgas analysis or sublance/drop sensor measurements are begun to finish the blow at the desired carbon and phosphorus content and temperature in the melt and the desired oxygen activity ( $\%FeO$ ) in the slag. The slag and metal composition are of course linked together. From this theoretical approach, it must be estimated that blowing patterns applied in BOF shops around the globe are following these general rules and the basic understanding of the process model.

Fig. 1 shows some schematic examples of actual blowing patterns applied in different plants. The converter tap weight size in this comparison ranges from 65 to 320 t, the

Table 1

**General Rules for Basic Oxygen Furnace (BOF) Blowing Patterns and Composition of Metal and Slag During the Blow**

BOF blowing patterns can be in general divided into seven to nine phases in which the lance height and (maybe) the oxygen flowrate must be adjusted to the required metallurgical steps. The phases to be recognized are:

Phase 0	Opening of the oxygen flow valve: At start of the blow, the oxygen valve is opened in two to three intermediate steps (70%, 90%, 100%) to avoid overshooting of the controller.
Phase I	Ignition: The selected starting lance height must be sufficient to guarantee bath penetration depth for immediate ignition on the one hand. On the other hand, damage of the lance tip caused by protruding scrap must be avoided.
Phase II	Slag formation (FeO): In the beginning of the blow, the lance is operated at a high level and with full oxygen flow to achieve sufficient FeO generation required for the quick lime solution. The total amount of the lime charge depends on the silicon content of the hot metal ( $Si_{HM}$ ). Due to this fact, the length of this period also depends on the $Si_{HM}$ . Early and quick slag formation is a key factor to reduce lance skull formation.
Phase III	Slag formation ( $SiO_2$ ): It is recommended to reduce the lance height at the end of the $Si_{HM}$ oxidation to keep the oxidation speed at a high level.
Phase IV	Dephosphorization ( $P_2O_5$ ): At the point of decreasing $Si_{HM}$ oxidation speed, dephosphorization at low metal/slag temperature starts. The speed of the phosphorus oxidation can be increased by reduction of the lance height. The length of this phase is between 500–800 $m_n^3$ oxygen depending on the size of the BOF vessel.
Phase V	Decarburization (high-speed $dC/dt$ ): The start of this phase is characterized by a maximum in the $CO_2$ curve and the strong incline of the CO curve in the offgas. In this phase, the critical path is to drive the lance quickly down to a position where the CO content of the gas reaches a level valuable for recovery (rich gas).
Phase VI	Decarburization (medium-speed $dC/dt$ ): The lance height must be adapted to the declining de-C speed.
Phase VII	Decarburization (low-speed $dC/dt$ ): The lance height must be further decreased to hold the CO content in the offgas as long as possible in the limits for gas recovery.
Phase VIII	Dynamic endpoint control (after sublance measurement): At the decline of the decarburization in many BOF shops, a sublance measurement for temperature and sampling is carried out. Based on this measurement, the heat is conditioned with cooling agent and oxygen or dynamic endpoint. During the sublance measurement, it is recommended that the oxygen flow (65% of the aim flowrate) be decreased to reduce the turbulences in the BOF. After the measurement, the oxygen flow is set back to the aim. In case of dry slag, it might be advantageous to increase the lance height slightly to increase the FeO content of the slag and to enhance dephosphorization at the end of the blow.
The bottom stirring flowrate is adjusted from the beginning (until the middle of the blow) at minimum flow to keep the plugs clear. At 75% of the blow, medium flowrates are adjusted. After the sublance measurement, the bottom gas rate is turned to maximum flow to promote bath mixing forces. The time for so-called “post-stirring” shall be adjusted to a minimum of 90 seconds.	

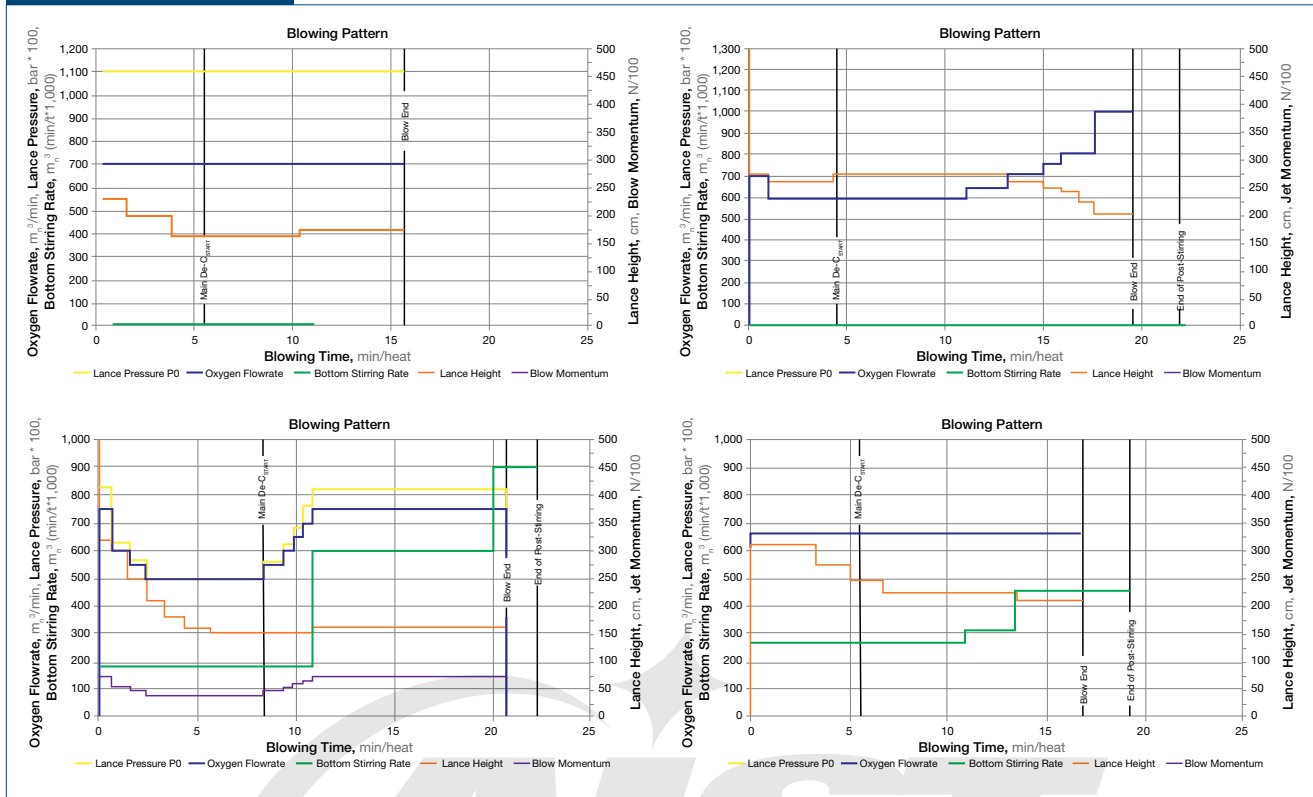
lance tip design from three to six holes with angles of 14–23°, and the final lance position ranges from 150 to 220 cm. Some plants operate with constant oxygen flow, others with progressive oxygen flow, and in some plants the flow is significantly decreased in the first half of the blow. The first two graphs in Fig. 1 show plants without bottom stirring. In the lower two graphs, plants with application of bottom stirring are shown. It becomes obvious that vigorous bottom stirring is applied in the second half of the blow and toward the blow end.

Comparing the profiles shown in Fig. 1, it is obvious that although the BOF process is a deeply investigated phenomena, with numerous researchers having investigated and published their results from lab, semi-industrial and industrial trials, the daily operation practice in the BOF shops is an empirical approach. It is rather based on control of undesired effects like lance and mouth skulling, slopping, visible emissions, and others than on model-based design of measurable parameters.

## Modeling the BOF Process

The general understanding of the BOF process is shown in Fig. 2. The oxygen jet dispatched from the multi-hole lance tip creates a cavity on the bath surface surrounded by a wave ridge. In this slag-free cavity, the oxygen jet reacts directly with the liquid metal inside the vessel. This area can be defined as the jet/bulk metal interface. The secondary effect induced by the jet is droplet generation and ejection toward the walls. There is some bulk slag above the bulk metal and between the wave ridge and the walls. In this area, a bulk slag/bulk metal interface determines the reactions. Most of the slag will be foamed to an emulsion generated by CO gas bubbles formed inside the bulk metal by oxidized metal droplets sinking back into the bath or by metal droplets being oxidized in the high (%FeO)-containing slag foam. Around the lance, there is a channel to release gas generated from the jet impact reaction to the mouth of the converter. This channel also is the main source for dust and iron sparks leaving the vessel into the offgas collecting

Figure 1

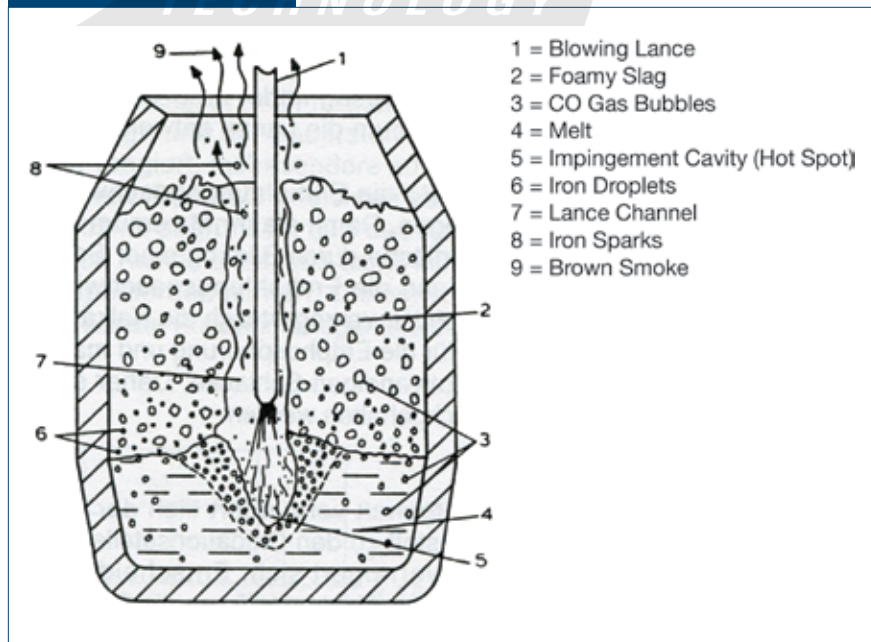


Comparison of various blow profiles from different plants.

system. The dominant role of the lance position and flow control is obvious.

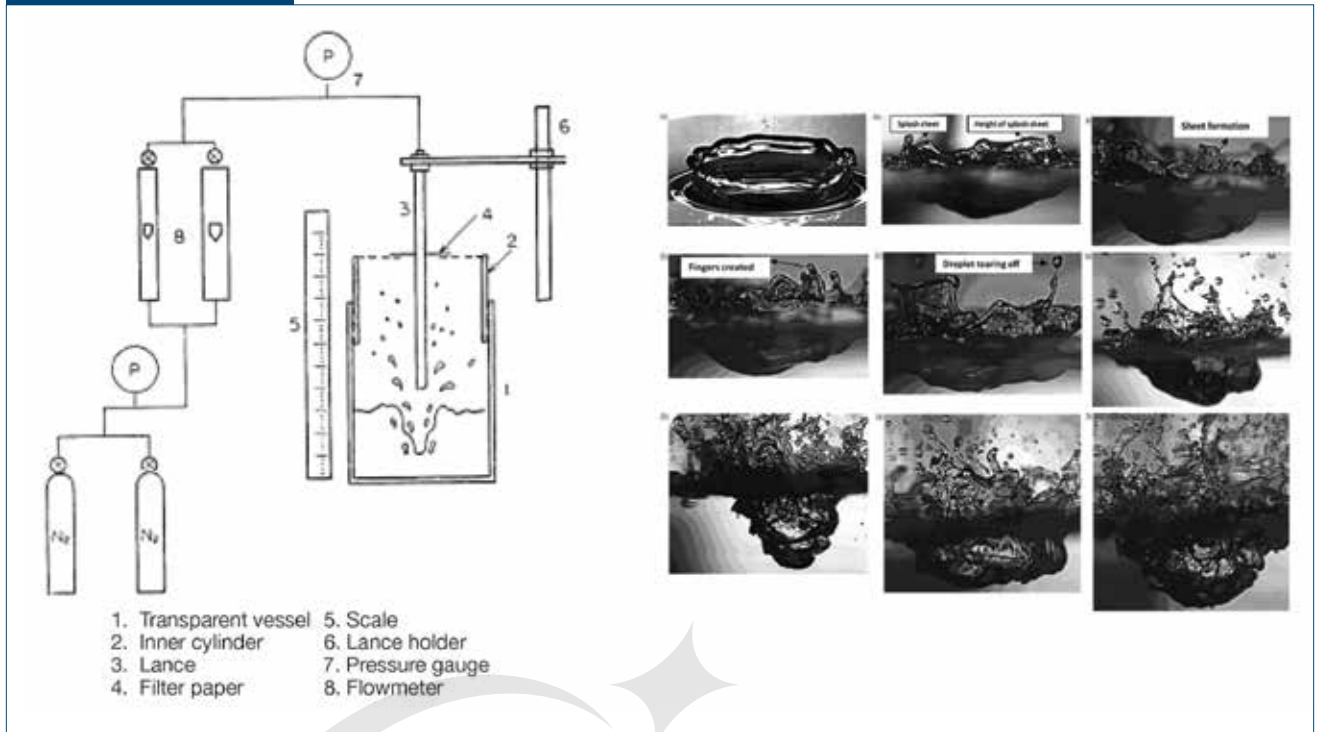
In this model, the operation of a bottom stirring system (low rates of 0.03–0.09  $\text{m}^3/\text{minute}/\text{ton}$ ) does not play any role in the initial stage of the blowing process. The low-flow bottom stirring is valuable in supporting bath mixing toward the end of the blow when the lance is already in the low position and the decarburization rate is rapidly declining. And it helps after the sublance measurement and during the post-stirring that equilibrium is achieved between bulk slag and bulk metal. The effect of higher bottom stirring rates (0.20–0.50  $\text{m}^3/\text{minute}/\text{ton}$ ) or bottom blowing rates by using oxygen is not included into the recent work.

Figure 2



Interface model concept during blowing of a basic oxygen furnace (BOF) vessel.

Figure 3



Penetration of an air/oxygen jet into a liquid surface in a cold lab-scale model.<sup>2,8</sup>

### Physical Modeling of the BOF Process

It is common practice to use thermochemical mass and heat balance models to operate the furnace. Charge materials and the oxygen amount are balanced to reach the aimed steel composition and temperature. Even today most of these models don't consider the physical effects of the lance blowing on the process results. The physical effects of the oxygen jet impinging on a liquid surface were investigated by numerous researches. In the initial stage as well as today (1954–2015), cold models are frequently used to study the effects of the jet at the bath surface (Fig. 3).<sup>1–10</sup>

Only a few researchers (1967–2005) have studied the mechanism of the blow in hot models (Fig. 4).<sup>11–14</sup>

Another possibility to study flow phenomena in a BOF during blowing is CFD (computational fluid dynamics) modeling, which today is widely applied. Fig. 5 shows the results from recent investigations.<sup>15,16</sup> All of the cold physical approaches (water models and CFD studies) do not consider or incompletely consider the influence of the slag layer on top of the metal bath and the effect of the chemical reactions and the temperature at the different transition areas. Today, it is well understood that the main part of the oxidation reactions during the blow happens inside of the slag foam above the bulk metal bath. Also, it is very clear

that the gas volume generated by the oxidation reactions at high temperature is much higher than can be simulated in a cold water model.

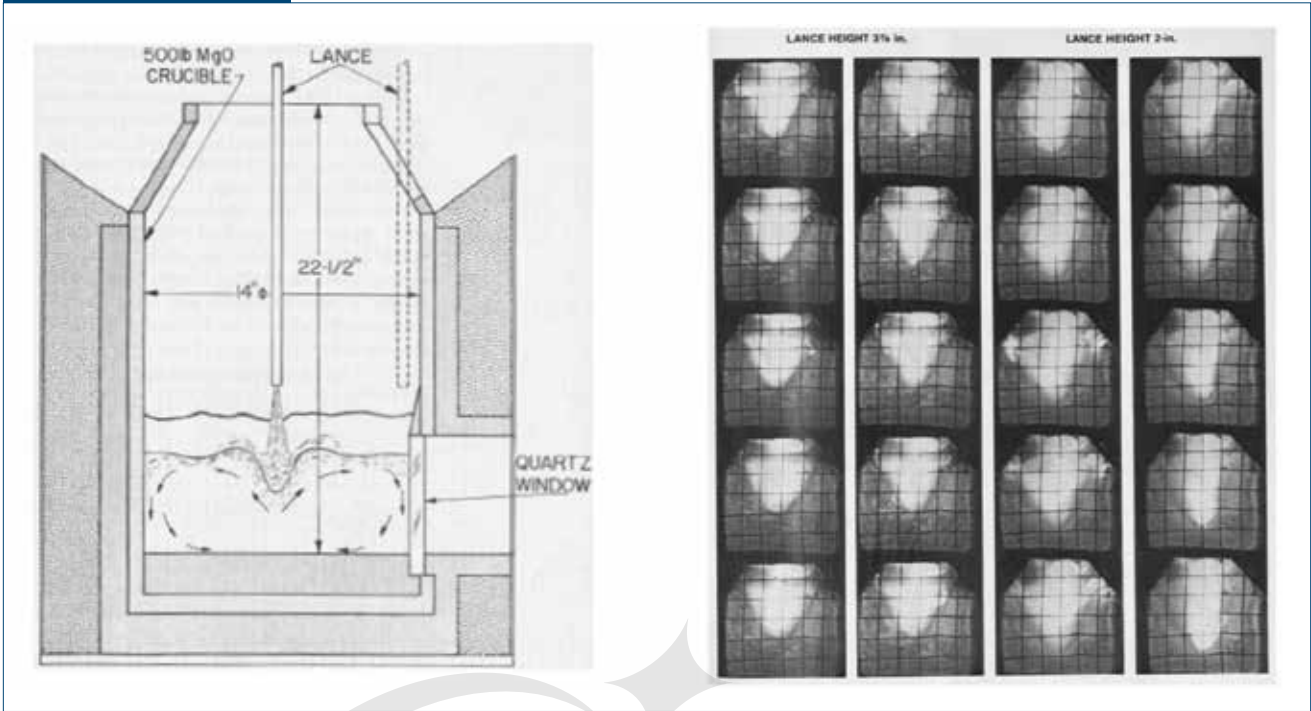
Hot models have the disadvantage that, in the small scale used, the observations during the blow are still limited due to the high-temperature reactions and process emissions hindering the visibility of the process. Nevertheless, from the hot models, important insight could be gathered about penetration depth, metal splash, and droplet size and generation amount.<sup>13</sup>

Fundamental studies and small-sized lab-scale trials are valuable in creating fundamental understanding of the BOF process, but the main question is how to translate this knowledge into blowing patterns for practical operational use. By application of dimensionless analysis, mathematical formulas have been developed to describe the effects of the blowing parameters (flowrate, lance height and nozzle design) on the change in the transition areas between metal, slag, droplets and foam, which will be discussed next.

### Mathematical Description of the Jet Penetration and Droplet Generation

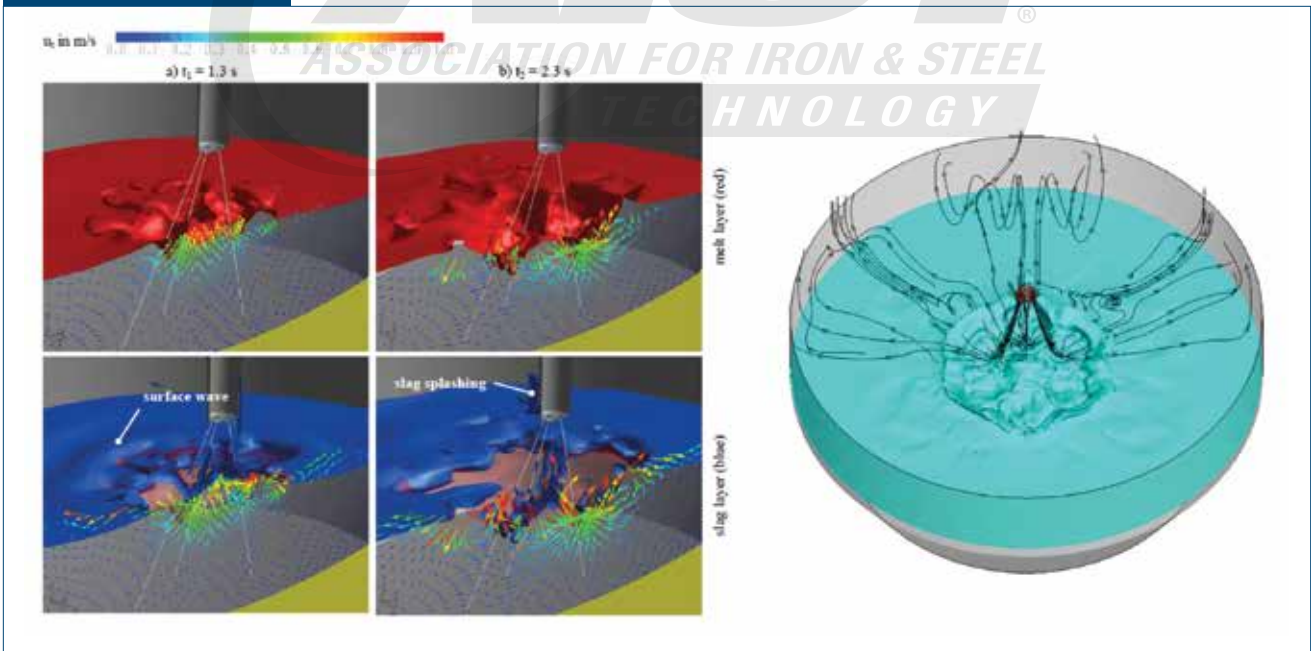
The common method to describe the effect of the oxygen jet on the surface of the metal bath is to

Figure 4



Penetration of an air/oxygen jet into a liquid surface in a hot lab-scale model.<sup>12</sup>

Figure 5



Modeling of jet penetration by computational fluid dynamics (CFD).<sup>15,16</sup>

calculate the so-called penetration depth or  $L$  [m], which is defined as the distance of the deepest point of the cavity to the bath surface in stationary condition. In dimensionless analysis, the penetration index (PI [-]), which is defined as the quotient of the penetration height  $L$  to the stationary bath height  $L_0$  [m], is applied. The equations published in the literature have three typical formats:

1. Equations derived from dimensionless analysis of water model trials (Collins and Lubanska,<sup>1</sup> Maia<sup>3</sup> and other).

$$\frac{\pi \cdot \rho_g \cdot v_m^2 \cdot d_E^2 \cdot \cos \theta \cdot n}{4 \cdot \rho_{LS} \cdot g \cdot h_L^3} = \frac{2}{K^2} \cdot \frac{h_n}{h_L} \cdot \left(1 + \frac{h_n}{h_L \cdot \cos \theta}\right)^2 \quad (\text{Eq. 1})$$

where

$\rho_g$  = gas density at nozzle exit in  $\text{kg/m}^3$ ,  
 $v_m$  = gas velocity at nozzle exit in  $\text{m/second}$ ,  
 $d_E$  = nozzle exit diameter in  $\text{m}$ ,  
 $\theta$  = nozzle angle in lance tip in  $^\circ$ ,  
 $n$  = number of nozzles in lance tip [n],  
 $\rho_{LS}$  = density of liquid steel in  $\text{kg/m}^3$ ,  
 $g$  = acceleration of gravity in  $\text{m/second}^2$ ,  
 $h_L$  = distance of nozzle to bath surface in  $\text{m}$ ,  
 $K$  = empiric constant [-] and  
 $h_n$  = penetration depth of the jet in  $\text{m}$ .

2. Empiric equations derived from water/hot model investigations (Flinn,<sup>11</sup> Ishikawa,<sup>2</sup> Masazumi (Segawa),<sup>4</sup> Kai<sup>5</sup> and other).

$$h_n = A_1 \cdot e^{\left(\frac{-0.78 \cdot h_L}{A_1}\right)} \quad (\text{Eq. 2})$$

$$A_1 = 63.0 \cdot \left(\frac{k \cdot \dot{V}_{O_2}}{60 \cdot n \cdot d_E}\right)^{\frac{2}{3}} \quad (\text{Eq. 3})$$

where

$h_n$  = penetration depth of the jet in  $\text{m}$ ,  
 $A_1$  = auxiliary variable,  
 $h_L$  = distance of nozzle to bath surface in  $\text{m}$ ,  
 $\dot{V}_{O_2}$  = oxygen flowrate [ $10^5 \text{ N/m}^2$ ],  
 $k$  = nozzle constant (1,056 for multiple hole lances),  
 $n$  = number of nozzle in lance tip [n] and  
 $d_E$  = nozzle exit diameter in  $\text{m}$ .

3. Simplified equations derived from regressions (Lange and Koria<sup>6,7</sup> and other).

$$\dot{M}_t = \frac{0.7854 \cdot 10^5 \cdot n \cdot d_t^2 \cdot P_{a_{real}} \cdot \left(1.27 \cdot \frac{P_0}{P_{a_{real}}} - 1\right)}{\rho_{LS} \cdot g \cdot h_L^3} \quad (\text{Eq. 4})$$

The vertical component of  $\dot{M}_t$  is the penetration depth:

$$\frac{h_n}{h_L} = 4.469 \cdot \dot{M}_h^{0.66} \quad (\text{Eq. 5})$$

$$\dot{M}_h = \dot{M}_t \cdot \frac{\cos \theta}{n} \quad (\text{Eq. 6})$$

The horizontal component of  $\dot{M}_t$  is the diameter of the cavity:

$$\frac{d_n}{h_L} = 2.813 \cdot \dot{M}_d^{0.282} \quad (\text{Eq. 7})$$

$$\dot{M}_d = \dot{M}_t \cdot \sin \theta \quad (\text{Eq. 8})$$

where

$\dot{M}_t$  = dimensionless jet impact in -,  
 $n$  = number of nozzles in lance tip [n],  
 $d_t$  = nozzle throat diameter [m],  
 $P_{a_{real}}$  = ambient pressure inside of the blowing converter [ $10^5 \text{ N/m}^2$ ],  
 $P_0$  = oxygen pressure at nozzle entrance in  $10^5 \text{ N/m}^2$ ,  
 $\rho_{LS}$  = density of the liquid in  $\text{kg/m}^3$ ,  
 $g$  = acceleration of gravity [ $\text{m/second}^2$ ],  
 $h_L$  = distance of nozzle to bath surface [m] and  
 $\theta$  = nozzle angle in lance tip [ $^\circ$ ].

For the result comparison of the equations, discussed as follows, the equation of Masazumi (Segawa)<sup>8</sup> was chosen for reference because this is the common equation used in many BOF shops in North and South America. The authors believe that the approach of Kai<sup>5</sup> is more complete, because in his publication in 1983,<sup>5</sup> for the first time the relation between the penetration index and the mixing energy dispatched by top and also bottom stirring/blowing was discussed. The equations of Lange and Koria<sup>6</sup> were chosen for reference because they have split the jet momentum

in a vertical and horizontal component. With the diameter and the depth of the cavity, the interface between the bulk metal and the oxygen jet can be calculated by application of the equation for the surface area of a parabola of revolution. The generation of droplets and their size distribution were investigated by Lange and Korla<sup>13</sup> in hot model trials carried out in the mid-1980s. In their laboratory tests, they splashed out metal droplets by blowing with a top lance onto a pool of liquid metal. After cooling down the metal collected on refractory material placed around the blowing vessel, they collected the solidified splashes and categorized them by screening. From this research work, equations to estimate the droplets generation (metal volume cycling) and the size distribution of the droplets were developed. The surface area of the interface between the metal droplets and the slag foam can be calculated from the amount and size of the droplets by application of the equation for the surface area of a sphere.

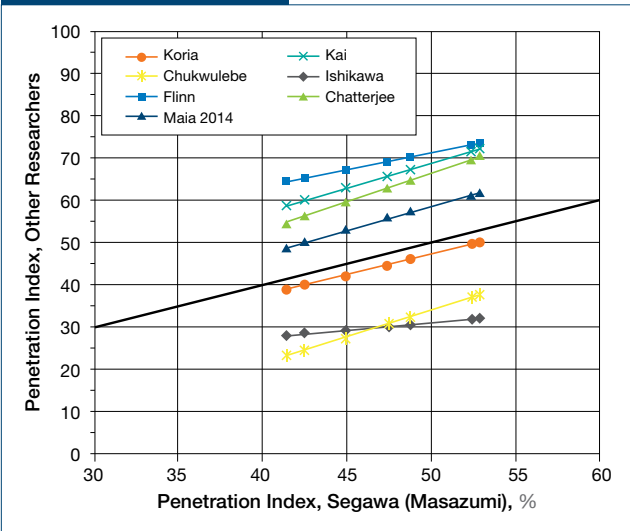
### Validation of Published Equations

To gain more confidence as to which formula should be used for future work, the equations of several researchers were used to calculate the penetration index for a typical BOF installation and lance design. The result is shown in Fig. 6, which compares the result obtained by the standard formula for the  $L/L_0$  relation by Masazumi (Segawa)<sup>4</sup> and the other equations. It is obvious that some formulas show the same behavior compared to the Segawa formula; others come to different trends. The best fits are the formulas of Lange and Korla<sup>6</sup> and Maia 2014.<sup>9</sup> The formula of Kai<sup>5</sup> has the same inclination but comes to significant higher penetration index numbers.

Another problem with the formulas of several researchers is that these formulas use an empiric tuning factor (nozzle factor  $k$ ) that was derived from water model trials. At the time of the trials, basically one to three nozzle lances with inclinations of 0–12° were used in BOF operations. Today, four to six nozzles are common operation practice and the nozzle angles vary from 14 to 23°. It is not possible to simply estimate the nozzle factor from past laboratory trials. So the common practice today is to freeze the nozzle factor at a constant value, which of course influences the results. To eliminate this problem, new water model trials with actual lance tip and nozzle configurations would be required. Therefore, the Ishikawa equation<sup>2</sup> and the Masazumi (Segawa) equation<sup>4</sup> are not recommended for use for blowing pattern design in the future anymore.

The next issue to be addressed for all existing equations was pointed out by Maia and Tavares<sup>10</sup> recently. All formulas calculate the penetration index is based

Figure 6



Various penetration index formulas compared to Segawa/Masazumi Validation.<sup>2-4,6,9,11,18</sup>

on a static bath height  $L_0$ . But in the BOF operation, the bath height is not static, it is dynamic:

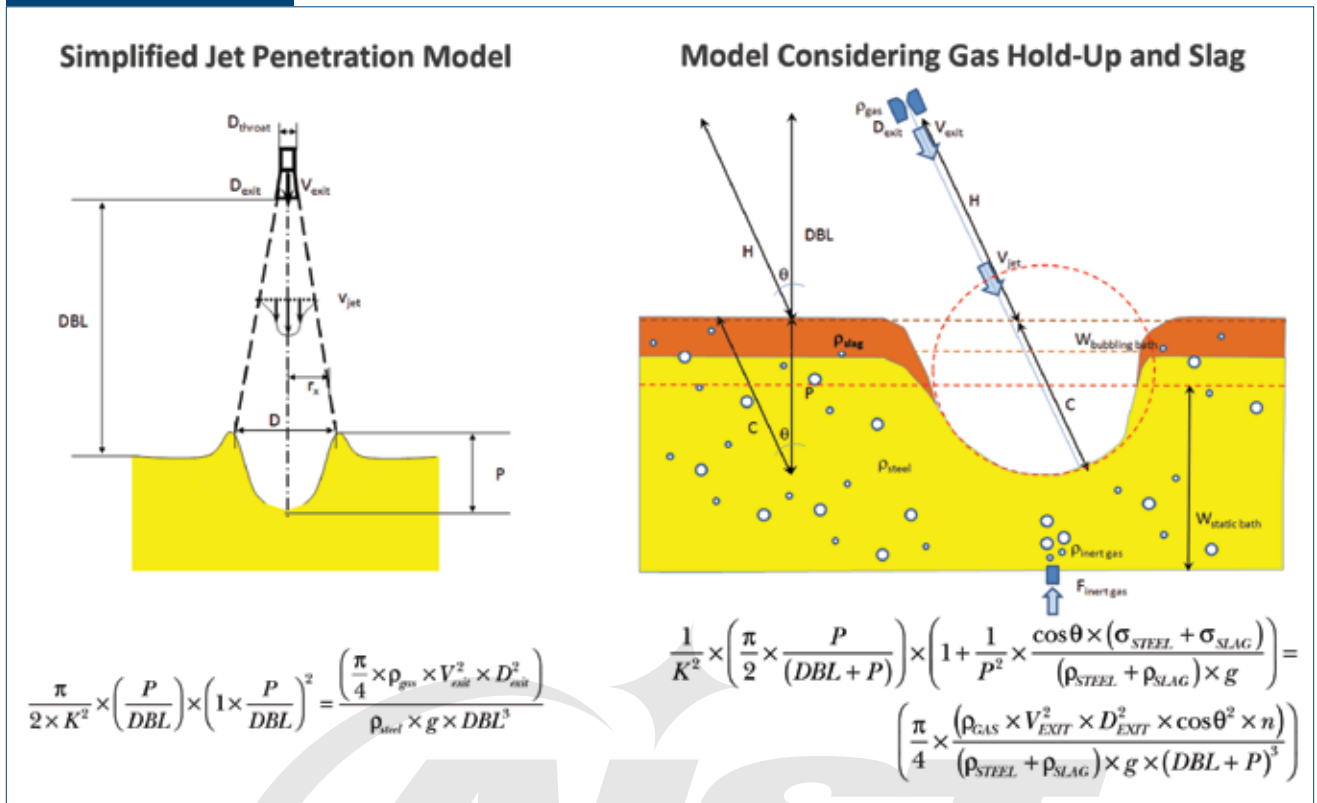
1. In most shops, the hot metal/scrap ratio varies according to price and availability. In general, these changes in the initial liquid's levels are not compensated in the blow patterns.
2. For the  $L/L_0$  calculation in most applications, the steel bath height from the refractory drawing is used. The bath height changes with the refractory wear are not corrected in the blow pattern, only in the lance position.
3. Oxidized metal droplets are sinking back into the melt and are being reduced by forming CO bubbles. These bubbles decrease the metal density and increase the metal bath height.
4. When bottom stirring is applied, Ar/N<sub>2</sub> bubbles are released to the melt. These bubbles will decrease the metal density and increase the bath height. Both effects are not recognized in the blow patterns.

The authors propose modifications of the penetration index formula, which are shown on the right side of Fig. 7. The influence of these effects on the results of the  $L/L_0$  theory must be further studied in water model experiments, especially the effects of the bottom stirring on the bath density.

### Interpretation of Penetration Index for Practical Use

The discussion of the validity of the  $L/L_0$  theory leads to the question "What is the practical benefit?" of the theoretical approach. The answer is obvious:

Figure 7



Jet penetration model modification requirements.<sup>9,10</sup>

The  $L/L_0$  theory is a theoretical model developed to provide a better understanding of the physical effects happening in a lance oxygen blowing vessel and combines the effects of flowrate changes and lance movements (lance tip nozzle design differences included). The results obtained from the laboratory trials have already been classified according to the physical effects observed in the past.<sup>4</sup> In Table 2,<sup>10</sup> the classical approach was more detailed and gives a classification and “translation” of the effects. Soft,

medium and hard blow are differentiated by the physical effects happening during blowing. The more intensive the blow, the more intensive the jet penetration, the splashing and the decarburization. However, this also leads to negative effects appearing such as lance, mouth and hood skulling.

But also, this consideration, same as the general rules for blowing patterns presented in Table 1, is more or less a general approach. Steelmakers design blow patterns to follow these general rules and to

Table 2

Jet Penetration Effect on Blowing Behavior<sup>10</sup>

Type of blow	$L/L_0$	Blow aspect
Oxidation	<0.20	Oxygen jet doesn't touch the static liquid bath, just creates atmospheric oxidation into the vessel
Soft	0.20–0.40	Small penetration
Soft-medium	0.40–0.55	Jet penetration is enough for ignition; able to start Fe oxidation and lime dissolution
Medium	0.55–0.60	Penetration applied to some De-C conditions for low P. Foaming slopping occurs in this range.
Medium-hard	0.60–0.75	Penetration applied in general during De-C blow period
Hard	0.75–0.80	Strong penetration, normally for fast De-C time. Metallic slopping occurs in this range.
Heavy	0.80–1.00	This relation is used to blow fast and save time; avoids bottom buildup. Dangerous for lance tip.
Furnace and lance damage	>1.00	This range is used for specific works outside the blow, like burn bottom



achieve the penetration index suitable for their operation. So the question arises: “How can the general figures be transformed into a practical approach?”

In Fig. 8, the calculation results of the characteristic parameters for an actual industrial case blowing pattern example are shown. In the upper graph, the oxygen flowrate [ $\text{m}^3/\text{minute}$ ], the lance height [cm], the oxygen pressure [bar] and the resulting jet momentum [N] are shown. Since the oxygen flow is kept constant and the lance tip design is also fixed, the pressure and the jet momentum are also constant during the blow. The lance height is changed sequentially to adapt to the different stages of the blow. In the first third of the blow, the lance is kept high to promote slag formation and lime/dolomite solution. At the estimated start of the main decarburization, the lance is kept on the lowest position, obviously not correlated to the amount of Si oxidation. After 50% of the blow, the lance is significantly raised to compensate for the slag reduction. Toward the blow end, the lance is driven down again to promote the final decarburization. Bottom stirring is not applied in this plant.

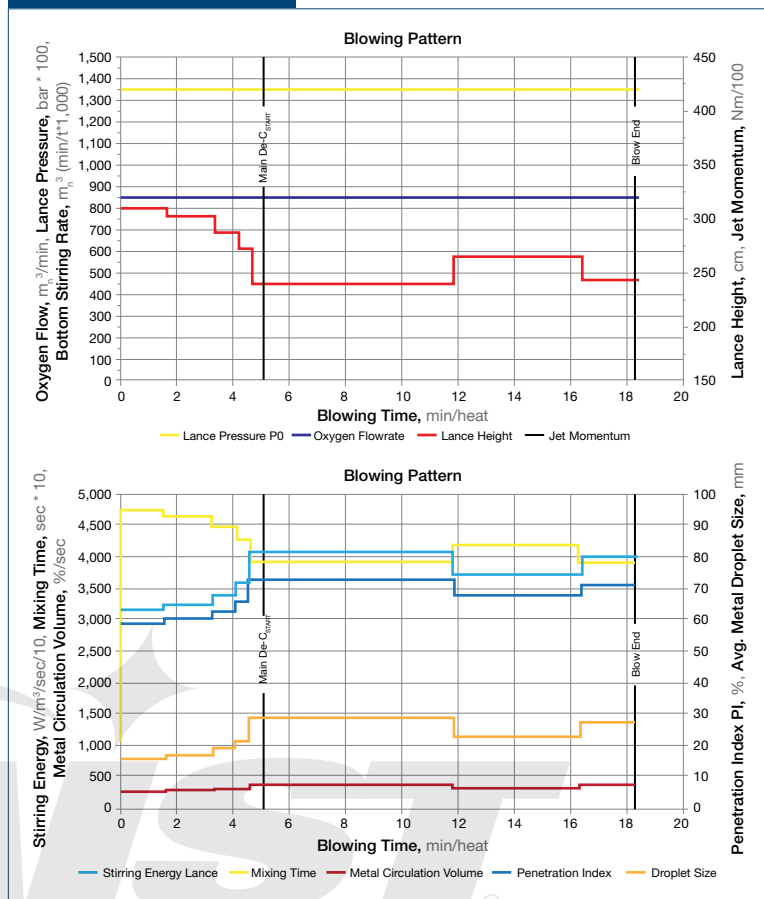
The “translation” of this blowing pattern into the characteristic formulas for jet penetration, stirring energy (just lance), mixing time, metal circulation volume and average droplet size is shown in the lower part of the diagram. Penetration index, mixing energy and also metal circulation volume follow the lance movement’s direct proportional. The droplet size also follows the PI and increases with PI. This means that the reaction interface of the droplets is inverse to the PI. The mixing time decreases with increasing mixing energy. From these results, the predominant influence of the lance position can be estimated.

Taking this interpretation into account, the multi-dimensional parameters of the blowing equipment can be reduced to only two main factors (Fig. 9):

1. The reaction interface of the oxygen jet to bulk metal.
2. The reaction interface of the metal droplets in the slag emulsion above the bulk metal bath.

The reaction interface between the oxygen jet and the bulk metal is created by the jet impingement to the surface created by the lance tip. The variables are clear: number of nozzles, nozzle inclination, nozzle throat diameter and nozzle exit diameter. These factors, together with the oxygen flowrate and the lance

Figure 8



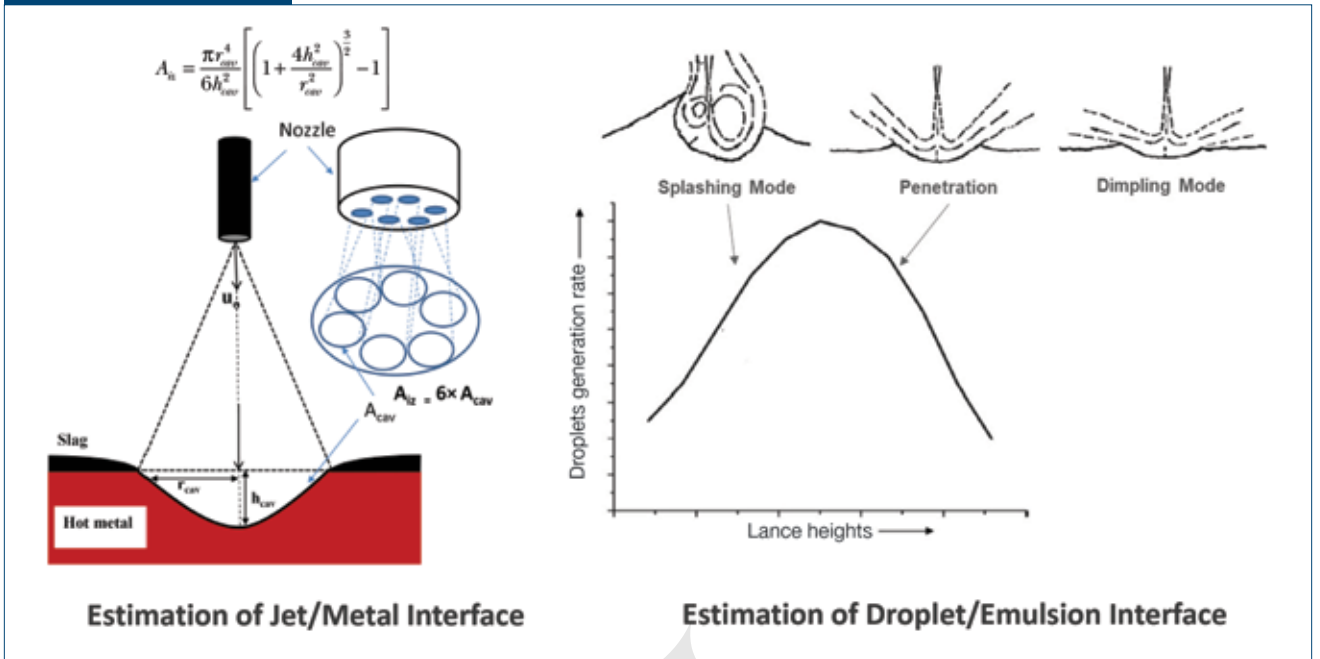
Results of jet penetration calculation at the BOF.

position above the bath, create the penetration cavity. Of course, in real industrial conditions, there will be not only one cavity but several cavities according to the number of nozzles in the lance tip. But for simplification reasons, it is estimated that the surface of the multiple cavities is equal to a single cavity. The reaction surface in this case can be calculated by a simple geometrical equation.

The reaction interface between the metal droplets ejected by the jet and the slag emulsion can be estimated by the calculation of the droplet “birth rate” and the average droplet diameter. Both parameters can be calculated by the equations developed by Lange and Korja.<sup>6</sup>

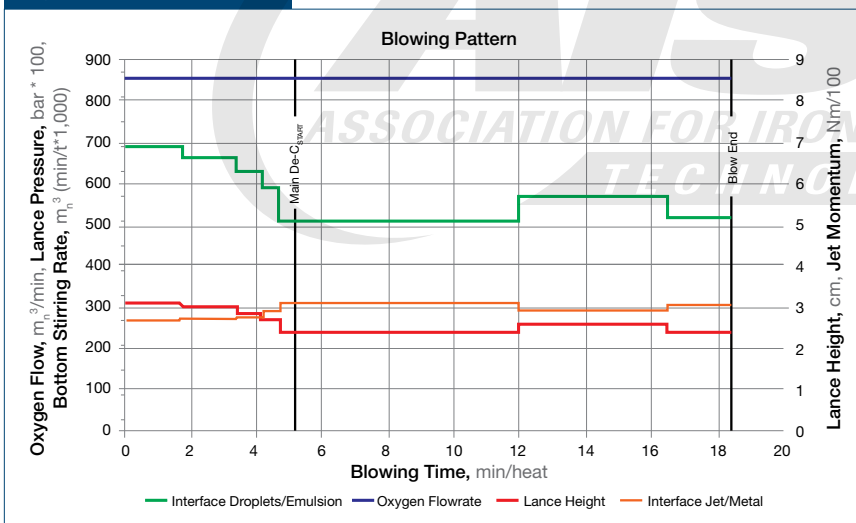
Again “translated” into the blowing pattern, the reaction interfaces show the behavior represented in Fig. 10. It becomes obvious that the oxygen jet/bulk metal interface behaves inversely to the lance height but the interface droplets/emulsion behaves directly. The figure also shows that the droplet interface is much higher (>200 times) compared to the jet/metal interface. In practical application, this indicates that lance height movements are much more efficient

Figure 9



Estimation of reaction interface changes.<sup>8</sup>

Figure 10



Blowing pattern and reaction interface changes.

compared to other manipulations to control the blowing process in oxygen steelmaking converters.

Fig. 11 shows the effects of a real blow on measurable input and output parameters. The upper left graph shows the blowing pattern execution (no constant oxygen flow applied). The upper right graph shows the offgas analysis (in the stack). The black curve is the decarburization rate in  $kg \text{ carbon}/m^3 \text{ oxygen}$ . The lower left graph shows the offgas volume and the lime, dolomite and iron ore addition, and the

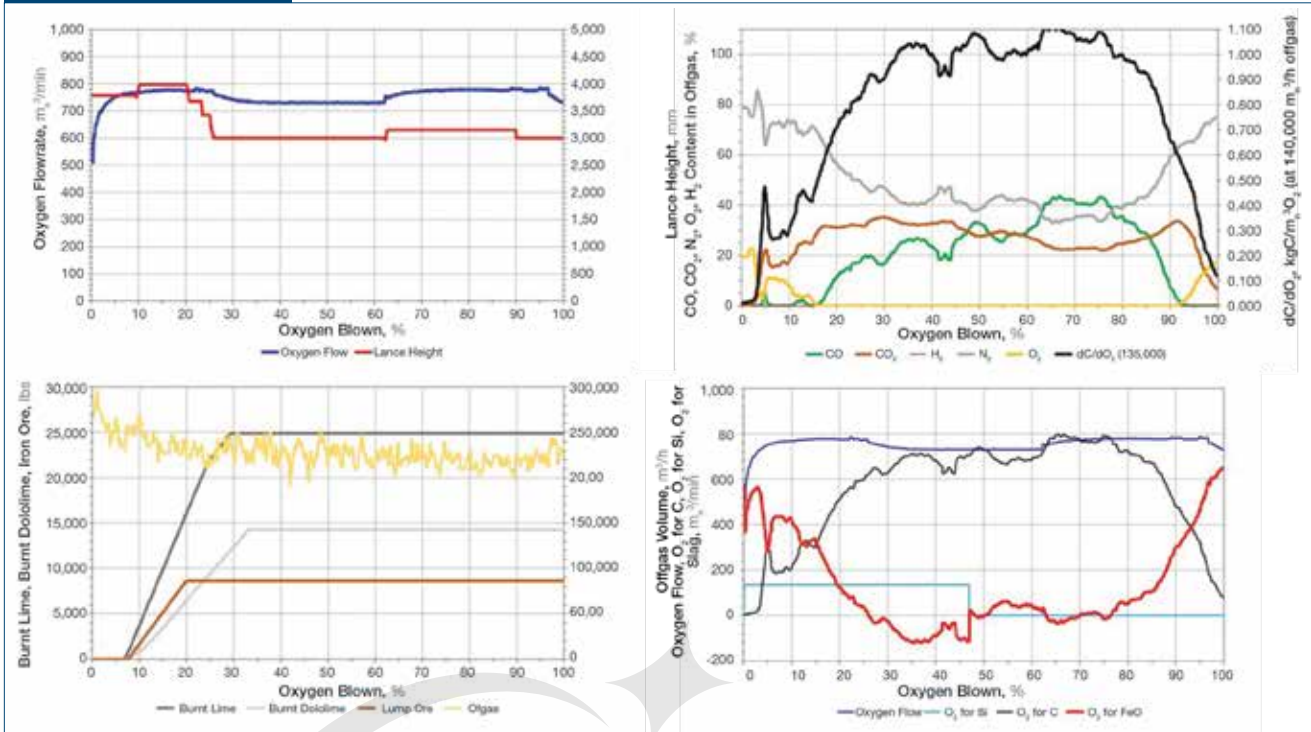
lower right side shows the estimated distribution of the blown oxygen to the predominant reactions.

The blowing regime is similar to the blow pattern in Fig. 8, but now showing the real-time data. The lance movement is according to the pattern; the oxygen flow is slightly reduced in the period of stopping. The offgas volume (including the infiltrated air) is at  $220,000 \text{ m}^3/\text{hour}$ . The addition of lime, dolomite and iron ore starts at roughly 90 seconds after the start of the blow. The offgas composition is shown in the upper right graph. The nitrogen content of the gas is decreasing from air level (69%) to blow level (40%) after 35% of the blow. After 80% of the blow, it raises back to air

level, which is almost reached at the end of the blow. CO starts increasing after  $O_2$  is gone and reaches up to 40% in the period when the lance is raised. At the point when  $O_2$  comes up at the end of the blow,  $CO_2$  is passing through a maximum that is typical for the blow. This means at this point of the blow, all gas coming from the vessel mouth is burnt by the infiltrated air to  $CO_2$ .

It can be clearly observed that in the lower right diagram, the red curve, the slag ( $\%FeO$ ) curve, turns

Figure 11



Blowing pattern and slag/gas reactions.

into negative values already in the middle of the desiliconization. In the authors' interpretation of the process, this effect is created by slag reduction of (%FeO), (%MnO) and (%P<sub>2</sub>O<sub>5</sub>); the slag dries out. If the (%FeO) content during this period falls below a level of 10%, the bulk slag will become solid. Gas is accelerated under the slag but cannot pass through. When the gas pressure under the solid slag is high enough to break the slag layer, it comes to an eruptive reaction, known as heavy slopping. When the slag dries out, this can also lead to splitting and skulling on the lance and furnace mouth.

The heavy slopping effect must not be confused with the overflow of liquid foaming slag, which is caused by the fact that the total foam volume simply is too big to keep the material inside the vessel. This overflow happens because the consistency of the slag is too viscous and the gas generation is already too high. It can be controlled by the lance position. To control the slag dry-out, the lance movement down to the lowest position must be delayed and adapted to the end of the desiliconization, which is at 45% of the blow in case a constant oxidation rate for silicon is estimated (the difference in reality is less than 10%).

Balajee et al.<sup>17</sup> reviewed the lance tip nozzle theory and design, and conducted BOF plant trials increasing the nozzle angle from 10 to 13° for improved slag formation and mixing. The lance and mouth skulling was decreased and allowed the BOF shop to utilize

low-silicon hot metal without adversely affecting the furnace lining wear. A wider nozzle angle reduced the jet overlap, minimizing the metal droplets hitting the furnace mouth and the lance surface that cause skulling. The lance life increased with the nozzle design modification, based on using the nominal BOF furnace pressure as the nozzle exit pressure and modifications to the blow profile to establish the desired L/L<sub>0</sub> penetration index range. The turndown performance (C and temperature) was improved.

Slopping was studied for two BOF steel shops by Chukwulebe<sup>18</sup> and Balajee.<sup>17</sup> Slopping index (SI) was correlated with a relative L/L<sub>0</sub> from the SI and the ratio of the furnace volume to charge volume (V), lance height (LH) and oxygen flowrate (OFR). A fuzzy logic model was developed using the major slopping variables, such as the HM Si, FeO/C and V. From the plant trials and data analysis, lance height and oxygen flowrate were adjusted to effectively control or minimize slopping during the sloop period (30–50% of the blow).

## Conclusions and Future Work

From the discussion of the blow physics and how to translate them into practical blowing patterns, it can be concluded:

1. The jet penetration equation of Koria and Lange is recommended as it does not use any adaptation factor K and takes into account the jet momentum and mixing energy.
2. The comparison of the blow physics with real-time operation results clearly demonstrates the predominant effect of lance height movements on the behavior of the bulk liquids and the emulsion during blowing. A complicated system of foam height control by consistency/viscosity control, bulk slag composition/fluidity control and CO gas generation control must be balanced during blowing.
3. It could be demonstrated that the metal droplet generation characterized by the amount and average size of the droplets and the reaction interface created by the droplets is the main effect produced from the oxygen jet and the lance position. The reaction interface metal droplets/emulsion is significantly higher compared to the direct reaction interface oxygen jet/bulk metal. By the lance movements, the metal droplets/emulsion interface is varied by half.

For future work, the authors recommend:

1. Modeling and real plant studies are needed to define the adaption factor K for the nozzle angles  $>12^\circ$  in jet penetration equations, including in the Masazumi (Segawa) equation, as currently, many BOFs use  $14$  to  $23^\circ$  nozzle angles, which was not common at the time the equations were published. Further, the effect of the number of the nozzles on the K factor should also be evaluated, taking into account the jet separation or the jet overlap phenomena.
2. The influence of the gas bubbles inside the metal bulk (generated from droplets falling back into the bath and from bottom stirring) on the metal density and the bath level must be studied.
3. In this study, the effect of bottom stirring on droplet birth rate was not discussed. Although droplet generation (birth rate) was investigated by other researchers, future modeling of the BOF process should focus on this effect. The metal droplet/emulsion interface influences the oxygen distribution between gas and slag and dependence on dynamic effects such as hot metal conditions (silicon content) and vessel profile during the campaign should be topics of study.

## References

1. R.D. Collins and H. Lubanska, "The Depression of Liquid Surfaces by Gas Jets," *Brit. J. Appl. Phys.*, Vol. 5, January 1954, pp. 22–26.
2. H. Ishikawa, S. Mizoguchi and K. Segawa, "A Model Study to Jet Penetration and Slopping in the LD Converter," *Tetsu-to-Hagané*, Vol. 58, No. 1, 1972, pp. 76–84.
3. A. Chatterjee, "On Some Aspects of Supersonic Jets of Interest in LD Steelmaking," *Iron and Steel International*, February 1973, pp. 38–40.
4. Masazumi, "Converter Steelmaking Process," European Patent specification No. 0017963 B1, 1980.
5. T. Kai, K. Okuhira, M. Higuchi and M. Hirai, "Cold Model Study of Characteristics in LD Converter With Bottom Blowing," *Transactions ISIJ*, Vol. 69, No. 2, 1983, pp. 42–51.
6. S.C. Koria and K.W. Lange, "Penetrability of Impinging Gas Jets in Molten Steel Bath," *Steel Research*, Vol. 58, No. 9, 1987, pp. 421–426.
7. S.C. Koria and K.W. Lange, "Estimation of Drop Sizes in Impinging Jet Steelmaking," *Ironmaking and Steelmaking*, Vol. 13, No. 5, 1986, pp. 236–240.
8. S. Sabah, G.A. Brooks and J. Naser, "Analysis of Splash Data From Oxygen Steelmaking," *AISTech 2013 Conference Proceedings*, Vol. II, 2013, p. 2083.
9. B.T. Maia, R.K. Imagawa, C.J. Batista, A.C. Petrucelli and R.P. Tavares, "Effects of Blow Parameters in the Jet Penetration by Physical Model of BOF Converter," *J. Mater. Res. Technol.*, Vol. 3, No. 3, 2014, pp. 244–256.
10. B.T. Maia, C.N.A. Diniz, G.G. Pereira, R.S. Salgado and R.P. Tavares, "Determination of the Mass in the Cold Model of the Bath Metal Slag by Supersonic Blow" (in Portuguese), *Steelworks Seminar International*, 2016.
11. R.A. Flinn, R.D. Pehlke, D.R. Glass and P.O. Hays, *Transactions of the Metallurgical Society of the American Institute of Mechanical Engineering*, Vol. 239, No. 11, 1967, p. 1176.
12. S.K. Sharma, J.W. Hlinka and D.W. Kern, "The Bath Circulation, Jet Penetration and High-Temperature Reaction Zone in BOF Steelmaking," *Iron & Steelmaking*, Vol. 4, 1977, pp. 7–18.
13. S.C. Koria and K.W. Lange, "Production of Drops in the Initial Stages of Basic Oxygen Steelmaking," *Proc. 3rd Int. Iron Steel Congress*, April 1978, pp. 373–385.
14. S.C. Koria, And K.W. Lange, "A New Approach to Investigate the Drop Size Distribution of BOF," *Steelmaking Met. Trans.*, Vol. 15B, 1984, pp. 109–116.
15. H.J. Odenthal, W.H. Emling, J. Kempken and J. Schluter, "Advantageous Numerical Simulation of the Converter Blowing Process," *AISTech 2007 Conference Proceedings*, Vol. I, 2007, pp. 1177–1193.
16. X. Zhou, "Numerical Simulation of the Interaction Between Supersonic Oxygen Jets and Molten Slag-Metal Bath in Steelmaking BOF Process," *Metallurgical and Materials Transactions*, Vol. 46B, June 2015.
17. S.R. Balajee, C.J. Bragg, S.M. Galloway and L.M. Keilman, "Oxygen Lance Design Modifications to Improve Lance Life and Performance at Inland's No. 2 BOF/CC Shop," *76th Steelmaking Conference Proceedings*, Vol. 76, 1993, pp. 145–161.
18. O.B. Chukwulebe, S.R. Balajee, K.J. Robertson, J.G. Grattan and M.J. Green, "Computer Optimization of Oxygen Blowing Practices to Control BOF Slopping," *AISTech 2004 Conference Proceedings*, Vol. I, 2004, pp. 751–762. ◆



This is an abridged version of a paper that was presented at AISTech 2018 — The Iron & Steel Technology Conference and Exposition, Philadelphia, Pa., USA. The original version was published in the Conference Proceedings.